Mol. Cryst. Liq. Cryst., Vol. 421, pp. 117–131, 2004

ISSN: 1542-1406 print/1563-5287 online
DOI: 10.1080/15421400490501635

ORIENTATIONAL DYNAMICS INDUCED BY CIRCULARLY POLARIZED LIGHT IN NEMATIC LIQUID CRYSTALS

Dmitry Krimer and Lorenz Kramer*
Physikalisches Institut der Universität Bayreuth, D-95440 Bayreuth, Germany

Gabor Demeter
Research Institute for Particle and Nuclear Physics of the Hungarian Academy of Sciences, Budapest, Hungary

We study theoretically the transitions induced by a circularly polarized plane light wave perpendicularly incident on a thin layer of homeotropically oriented nematic liquid crystal. There are three dynamical regimes separated by different types of transitions.

Keywords: nematic liquid crystals; nonlinear optics; orientational transitions

I. INTRODUCTION

An interesting optical phenomenon demonstrated by nematic liquid crystals (NLCs) called self-induced stimulated light scattering (SILS) was a subject of intensive study during the last two decades. It is known that the NLC is an anisotropic uniaxial medium with the optical axis parallel to the local molecular distribution described by the director $\mathbf{n}(\mathbf{r},t)$. When the light propagates through the NLC, its electric field exerts a torque on the molecules that can cause collective molecular reorientation. The light polarization inside the NLC layer is also changed because of birefringence. These two effects together can give rise to interesting phenomena such as persistent rotation of the molecules in SILS.

As is known for some time, circularly polarized light incident normally on a homeotropically aligned NLC film induces a first-order Freedericksz

This work was supported by DFG Grant No. KR690/16-1 and RTN contract HPRN-CT-2002-00312 funded by EU.
*Corresponding author. Tel.: +49921-55-3255; E-mail: Dmitry.krimer@uni-bayreuth.de

transition (at some critical value of intensity) leading to a reoriented state with uniform director precession [1]. This effect is well understood and can be interpreted in terms of angular momentum transfer from the light to the medium. Since the collective molecular rotation dissipates energy, the light beam has to transmit part of its energy to the medium. As the NLC is a transparent medium this energy loss leads to a red shift of part of the light beam [2,3]. With further increase of light intensity a transition to a more complex rotating state with a nutation-type motion of the director has recently been observed [4,5]. Here we investigate theoretically the light-induced instabilities and the regimes of director motion as a function of light intensity.

II. THEORETICAL MODEL

We consider a circularly polarized plane wave incident perpendicularly on a layer of nematic LC that has initially homeotropic alignment (with strong homeotropic anchoring at the boundaries). The light is polarized in the plane of the layer (the (**x,y**) plane) and propagates along the positive **z**-axis (see Fig. 1). We assume that the diameter of the laser beam is much larger than the thickness of the layer, and consider the case when the

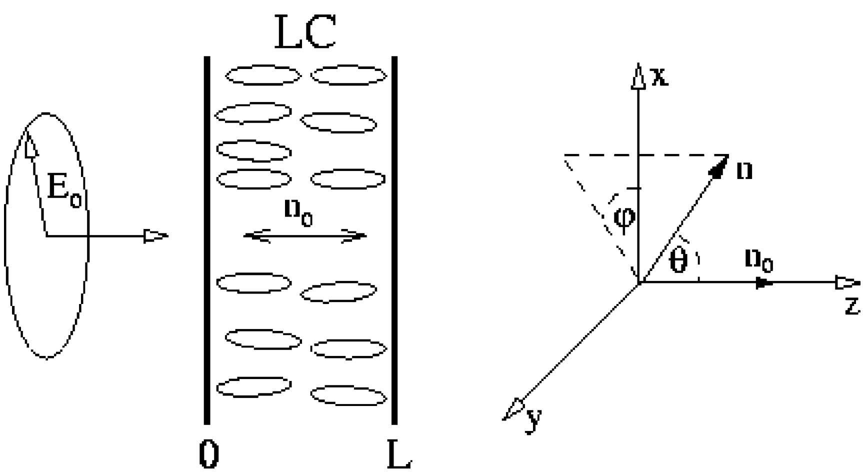

FIGURE 1 Geometry of the setup: circularly polarized light incident perpendicularly on a nematic LC layer with the director $\mathbf{n}_0 \,||\, \mathbf{z}$ (homeotropic state). The components of the director n are described in terms of the angles θ, φ ($\theta = 0$ in the homeotropic state).

director depends only on z, t. Then the light inside the nematic can be treated as a plane wave. We introduce the spherical angles $\theta(z,t)$ and $\varphi(z,t)$ to describe the director $\mathbf{n} = (\sin\theta\cos\varphi, \sin\theta\sin\varphi, \cos\theta)$.

The electric field is governed by Maxwell's equations. These equations contain the dielectric tensor that depends on the director components:

$$\varepsilon_{ij} = \varepsilon_{\perp}\delta ij + \varepsilon_a n_i n_j, \tag{1}$$

where $\varepsilon_a = \varepsilon_{||} - \varepsilon_{\perp}$ is the dielectric anisotropy and $\varepsilon_{\perp}(\varepsilon_{||})$ is the dielectric permittivity perpendicular (parallel) to $\mathbf{n}$. We write the electric field in the form: $\mathbf{E}(\mathbf{r},\mathrm{t}) = 1/2(\mathbf{E}(z,t)\mathrm{e}^{-\mathrm{i}\,\omega\,\mathrm{t}} + \mathrm{c.c.})$, where $k_0 = \omega/c$ is the wave-number in vacuum and $\mathbf{E}(z,t)$ is the amplitude that varies slowly in time compared to ω^{-1} and obeys the equation:

$$\frac{\partial^2\mathbf{I}}{\partial z^2} = -\frac{k_0^2}{\varepsilon_{zz}}\mathbf{MI} \tag{2}$$

where

$$\mathbf{M} = \begin{pmatrix} \varepsilon_{xx}\varepsilon_{zz} - \varepsilon_{xz}^2 & \varepsilon_{xy}\varepsilon_{zz} - \varepsilon_{xz}\varepsilon_{yz} \\ \varepsilon_{xy}\varepsilon_{zz} - \varepsilon_{xz}\varepsilon_{yz} & \varepsilon_{yy}\varepsilon_{zz} - \varepsilon_{yz}^2 \end{pmatrix}, \quad \mathbf{I} = \begin{pmatrix} E_x \\ E_y \end{pmatrix}.$$

The z component of the electric field can be found from the following relation:

$$E_z = -\frac{\varepsilon_{xz}E_x + \varepsilon_{yz}E_y}{\varepsilon_{zz}}. \tag{3}$$

We may now perform the transformation from the basis $(\mathbf{e}_\mathrm{x},\mathbf{e}_\mathrm{y})$ into the local basis $(\mathbf{e}_\mathrm{o},\mathbf{e}_{\mathrm{e}\perp})$ where the matrix $\mathbf{M}$ has a diagonal form [6]. In this new coordinate system the field components are the amplitudes of the ordinary E_o and extraordinary $E_{e\perp}$ waves in the $(\mathbf{x},\mathbf{y})$ plane, respectively, related to E_x, E_y as follows:

$$\psi = \mathbf{OI}, \tag{4}$$

where

$$\mathbf{O} = \begin{pmatrix} -\sin\varphi & \cos\varphi \\ \cos\varphi & \sin\varphi \end{pmatrix} \quad \text{and} \quad \psi = \begin{pmatrix} E_\mathrm{o} \\ E_{e\perp} \end{pmatrix}.$$

Introducing dimensionless $z \to z\pi/L$, $k_0 \to k_0 L/\pi$ (L is the thickness of the layer) and rewriting Eq. (2) in terms of E_o, $E_{e\perp}$ under the geometric optics approximation ($k_0 >> 1$), the equations for the ordinary and extraordinary waves can be derived:

$$\begin{cases} A_o' = -\varphi' \sqrt{\frac{\lambda_e}{\lambda_o}} e^{i\alpha(z)} A_e \\ A_e' = -\frac{\lambda_e' A_e}{4\lambda_e} + \varphi' \sqrt{\frac{\lambda_o}{\lambda_e}} e^{-i\alpha(z)} A_o \end{cases} \tag{5}$$

Here the prime marks the derivative with respect to z ($0 \leq z \leq \pi$). A_o, A_e are amplitudes that vary slowly with z on the scale k_0^{-1} and are defined by

$$E_o = A_o \cdot e^{ik_0\sqrt{\lambda_o}\cdot z}, \quad E_{e\perp} = A_e \cdot e^{ik_0 \int_0^z dz' \sqrt{\lambda_e(z')}} \tag{6}$$

and

$$\lambda_0 = \varepsilon_\perp, \; \lambda_e = \frac{\varepsilon_\perp(\varepsilon_a + \varepsilon_\perp)}{\varepsilon_\perp + \varepsilon_a n_z^2}, \quad \alpha(z) = k_0 \int_0^z \left(\sqrt{\lambda_e} - \sqrt{\lambda_o}\right) dz' \tag{7}$$

Here $\alpha(z)$ is the phase delay induced by the nematic between the ordinary and extraordinary waves.

The boundary conditions for the amplitudes A_o, A_e (normalized to the amplitude of the incoming light) at $z = 0$ are:

$$|A_{e0}|^2 = |A_{o0}|^2 = \frac{1}{2}, \; A_{e0}A_{o0}^* = \pm\frac{i}{2}, \tag{8}$$

where the sign in Eq. (8) defines the helicity of the incident light.

The equations for θ and φ are obtained from the equations of motion of the director **n**, which include the elastic, electromagnetic and viscous torques [7]:

$$\begin{aligned} \frac{\partial\varphi}{\partial t} &= \frac{1}{\sin^2\theta}\frac{\partial}{\partial z}[(1-(1-k_2)\sin^2\theta)\sin^2\theta\varphi'] \\ &\quad + 2\rho\frac{\lambda_e}{\lambda_o}\mathrm{Re}[A_e A_o^* e^{i\alpha(z)}] \quad \frac{\partial\theta}{\partial t} = (1-(1-k_1)\sin^2\theta)\theta'' \\ &\quad - \frac{\sin 2\theta}{2}\Big[(1-k_1)\theta'^2 + (1-2(1-k_2)\sin^2\theta)\varphi'^2 \\ &\qquad - 2\rho\left(\frac{\lambda_e}{\lambda_o}\right)^2 |A_e|^2\Big] \end{aligned} \tag{9}$$

Here $k_1 = K_1/K_3$, $k_2 = K_2/K_3$ where K_1, K_2, K_3 are, respectively, the splay, twist and bend elastic constants of the LC [7]. In Eq. (9), time t is normalized to the characteristic relaxation time τ of the director and $\rho = I/I_c$ is dimensionless incident light intensity wth

$$\tau = \frac{\gamma_1 L^2}{\pi^2 K_3}, \quad I_c = \frac{2\pi^2}{L^2}\frac{c(\varepsilon_\perp + \varepsilon_a)K_3}{\varepsilon_a\sqrt{\varepsilon_\perp}} \tag{10}$$

where γ_1 is an effective rotational viscosity and $I_c/2$ is the threshold intensity of the light induced Freedericksz transition (LIFT) for linearly polarized light at perpendicular incidence.

The boundary conditions for θ, φ are (strong homeotropic anchoring):

$$\varphi'_{z=0,\pi}(t) = 0, \quad \theta_{z=0,\pi}(t) = 0 \tag{11}$$

It should be noted that the coupled director and field equations (5), (9) together with the boundary conditions (8), (11) are invariant with respect to rotations around the z-axis $\varphi \to \varphi + \delta\varphi$ (as a consequence of isotropy in ($\mathbf{x}$,$\mathbf{y}$) plane).

The field equations (5) may be solved by means of successive iterations assuming that $|\varphi'| < 1$ (not too large gradient of the twist distortion). The zeroth-order solution of Eq. (5) is given by:

$$A_o^{(0)} = A_{o0}, \quad A_e^{(0)} = A_{e0}\left(\frac{\lambda_o}{\lambda_e}\right)^{\frac{1}{4}} \tag{12}$$

and the recurrence relations for the solution after the m iterations has the following form:

$$\begin{cases} A_o^{(m)} = A_{o0} - \int\limits_0^z dz'\varphi'\sqrt{\frac{\lambda_e}{\lambda_o}}e^{i\alpha(z')}A_e^{(m-1)} \\ A_e^{(m)} = A_{e0} - \int\limits_0^z dz'\frac{\lambda_e' A_e^{(m-1)}}{4\lambda_e} + \int\limits_0^z dz'\varphi'\sqrt{\frac{\lambda_o}{\lambda_e}}e^{-i\alpha(z')}A_o^{(m-1)} \end{cases} \tag{13}$$

The result after m iterations can be substituted into the evolution equations (9).

We then expand θ and φ with respect to z in systems of orthogonal functions (similar to [8]) which satisfy the boundary conditions (11):

$$\theta = \sum_{n=1}\theta_n(t)\sin nz, \quad \varphi = \varphi_0(t) + \sum_{n=1}\varphi_n(t)\frac{\sin[(n+1)z]}{\sin z} \tag{14}$$

The zeroth mode $\varphi_0(t)$ in Eq. (14) does not depend on z and describes the pure rotation of the director (without elastic distortion) around the

z-axis. After substituting the expansions (14) into Eqs. (9) and projecting on the modes of expansion (Galerkin method), a set of coupled nonlinear ODE-s for the modes $\theta_n(t)$, $\varphi_n(t)$ is obtained. We have solved these equations numerically, choosing the number of modes and iterations for A_o, A_e such that the accuracy of the calculated director components was better than 1%.

As a result of isotropy, the ODE for $\varphi_0(t)$ is decoupled from the rest and from the boundary conditions Eqs. (8) and (11). This is the case only for circularly polarized incident light.

In the calculations, we used the material parameters for the nematic *E7* (at room temperature): $K_1 = 11.09 \times 10^{-7}$ dyn, $K_2 = 5.82 \times 10^{-7}$ dyn, $K_3 = 15.97 \times 10^{-7}$ dyn, [8], $n_e = 1.746$, $n_o = 1.522$ [9] (refractive indices of the ordinary and extraordinary light, respectively), $\lambda = 532\,\text{nm}$ (wavelength

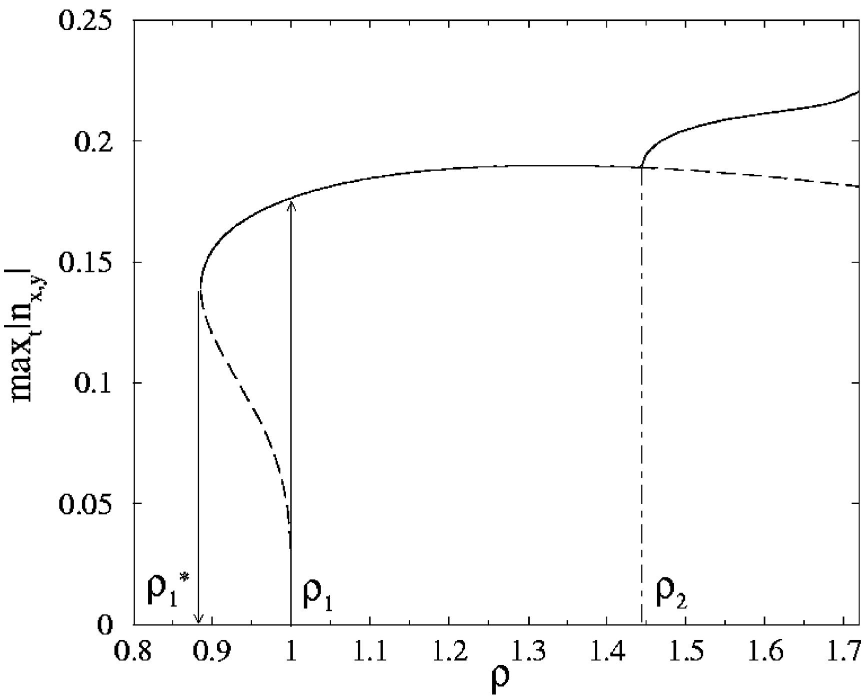

FIGURE 2 Maximum of the director components n_x, n_y with respect to t at point $z = \pi/2 - 0.1$ inside the nematic layer versus normalized intensity ρ. Solid (dashed) lines are stable (unstable) solutions. At $\rho = \rho_1$: transition to the regime of uniform director precession; at $\rho = \rho_1^*$: switch back to the homeotropic state; at $\rho = \rho_2$: transition to the regime of nonuniform director precession.

of laser), $\gamma_1/K_3 = 10^6 \mathrm{s\,cm}^{-2}$ [10]. The calculations were made for a layer of 100 μm thickness. For these parameters $I_c \approx 2.6\,\mathrm{kW/cm}^2$, $\tau \approx 10\,\mathrm{s}$.

III. FIRST REGIME OF UNIFORM DIRECTOR PRECESSION

As demonstrated in [1] the homeotropic state remains stable when the incident light intensity is below some critical value ($\rho_1 = 1$ in normalized units). Above the threshold ρ_1 the system settles in a state of uniform precession of the director around the z-axis (UP1). This regime was analyzed in [3] where the approximate value for the frequency of precession and the transcendental equation for the phase delay $\delta \equiv \alpha(z = \pi)$ were found.

Let us start with the analysis of the UP1 regime where $\varphi_0(t)$ grows linearly in time and the rest of the modes φ_n, θ_n ($n = 1, \ldots$) do not depend on t: $d\varphi_n/dt = d\theta_n/dt = 0$. Thus, in this case, we must solve a set of nonlinear algebraic equations on φ_n, θ_n that is decoupled from the evolution equation for φ_0. After solving these equations numerically and substituting φ_n, θ_n to

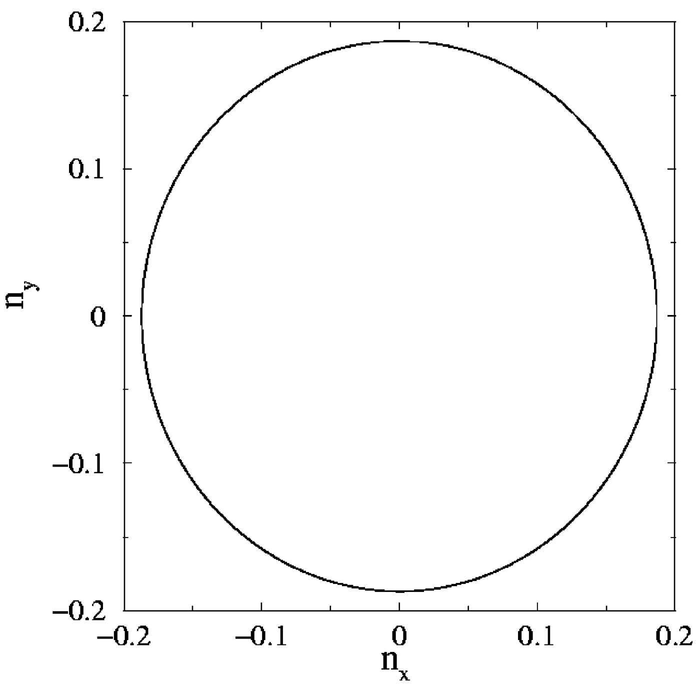

FIGURE 3 Limit cycle in the (n_x,n_y) plane at $\rho = 1.15$.

the equation for $\varphi_0(t)$, the frequency $2\pi f_0 = d\varphi_0/dt = const$ of the uniform precession is found.

In Figure 2 the maximum of the director components $max_t|n_x, n_y|$ with respect to t at point $z = \pi/2$-0.1 inside the nematic versus intensity ρ is plotted. As is seen from the figure at $\rho = \rho_1$ we deal with a first-order Freedericksz transition (subcritical Hopf bifurcation) with a hysteresis. If one starts from the UP1 state and the intensity ρ is decreased, the director (ideally) switches back to the homeotropic state at some lower values of intensity $\rho_1^* \approx 0.88$ where a saddle-node bifurcation occurs (see Fig. 2).

In Figure 3 a limit cycle of the time evolution of the director is shown in the (n_x, n_y) plane at $z = \pi/2$-0.1 for $\rho = 1.15$. It is represented by a simple circle. Clearly, in the rotational coordinate system (which rotates around z-axis with a frequency f_0) this state is a fixed point.

In Figure 4 the typical time Fourier spectra of n_x, n_y and of the output intensities $|E_x|^2$, $|E_y|^2$ are depicted for the UP1 regime. In both spectra only one peak is present. The frequency of the uniform oscillations of $|E_{x,y}|^2$

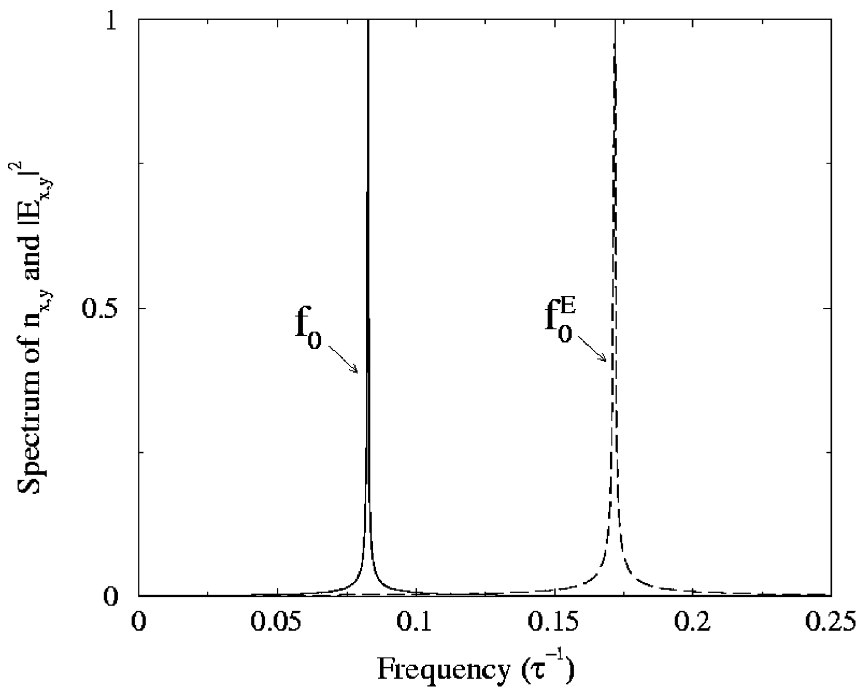

FIGURE 4 Spectra of n_x, n_y and output intensities $|E_x|^2$, $|E_y|^2$ at $\rho = 1.15$. Amplitudes of the peaks are in arbitrary units.

(around some nonzero values) is $f_0^E = 2f_0$, since the angle ϕ enters quadratically into the expressions for $|E_{x,y}|^2$:

$$|E_x|^2(|E_y|^2) = \cos^2\varphi|A_e|^2 \pm \sin 2\varphi \mathrm{Re}[A_e A_0^* e^{i\alpha(z)}] + \sin^2\varphi|A_o|^2$$
$$E_x E_y^* + E_x^* E_y = \sin 2\varphi(|A_e|^2 - |A_0|^2) + 2\cos 2\varphi \mathrm{Re}[A_e A_0^* e^{i\alpha(z)}] \tag{15}$$

As seen from Figure 2, the frequency f_0 eventually decreases with increasing light intensity (see Sec. V and [3]).

IV. REGIME OF NONUNIFORM DIRECTOR PRECESSION

As demonstrated experimentally in recent papers, and partially explained theoretically [4,5], with further increase of the light intensity one reaches a critical value where the director starts to precess nonuniformly. We found that the UP1 state becomes unstable in a secondary supercritical Hopf

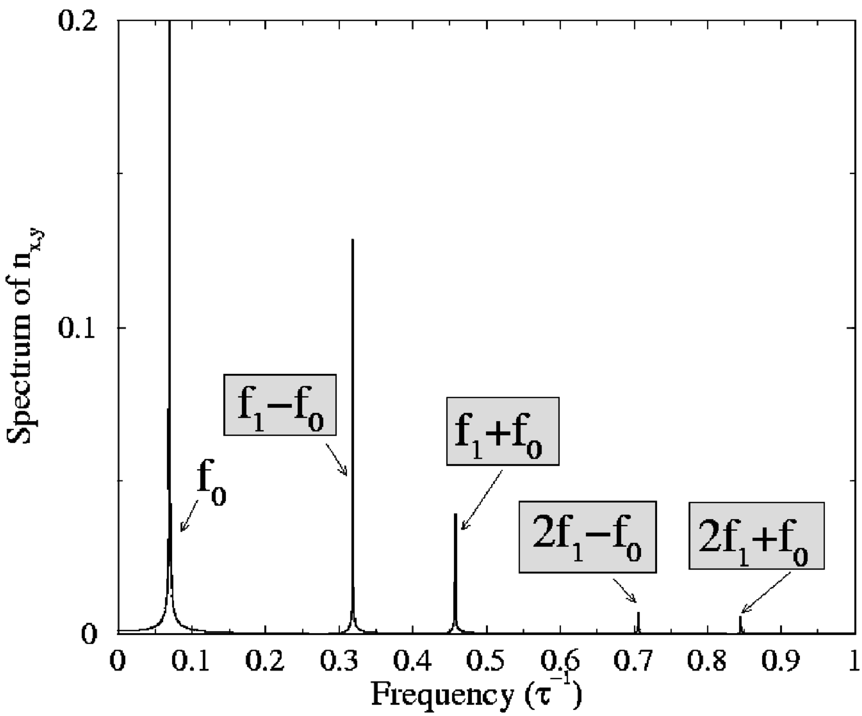

FIGURE 5 Spectrum of n_x, n_y at $\rho = 1.55$. Amplitudes of the peaks are normalized to the first peak in the spectrum.

bifurcation at $\rho_2 \approx 1.45$ and at $\rho > \rho_2$. The phenomenon can be traced back to the onset of a nutation-type motion of the director. We will call this state a state of nonuniform precession of the director (NUP). In this regime all modes $\theta_n(t)$, $\varphi_n(t)$ are time dependent and a new frequency f_1 (associated with the nutation) appears in the time Fourier spectrum of $n_{x,y}$ and $|E_{x,y}|^2$. We solved the set of the evolution equations on modes. It was necessary to retain at least six modes of both angles and six iterations for A_o, A_e to obtain the solution with an accuracy better than 1%.

In Figure 2 (upper solid line) the maximum of the director components n_x, n_y versus intensity ρ for the NUP regime is depicted. As indicated on the figure, at $\rho > \rho_2$ the UP1 state is unstable (dashed line).

The Fourier spectrum of the oscillating part of φ_m, θ_m $[m = 1, \ldots]$ contains frequencies nf_1, where n is an integer. The frequencies of the spectra of n_{xy} and $|E_{xy}|^2$ are given by the simple formulas (f_0, $n f_1 \pm f_0$) and ($f_0^E, nf_1 \pm f_0^E$) respectively, where $f_0^E = 2f_0$. Actually, the

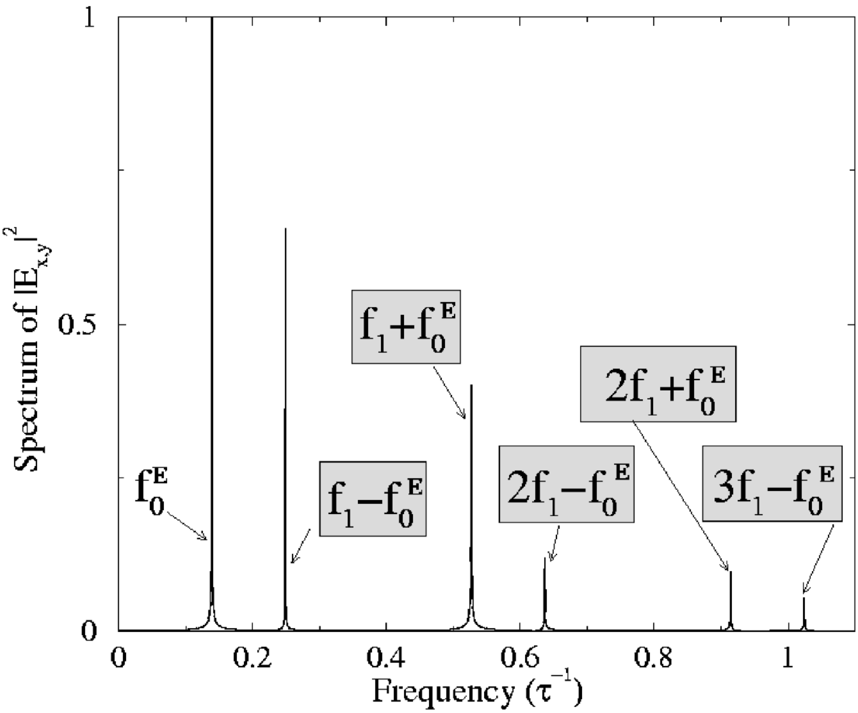

FIGURE 6 Spectrum of $|E_x|^2$, $|E_y|^2$ at $\rho = 1.55$. Amplitudes of the peaks are normalized to the first peak in the spectrum.

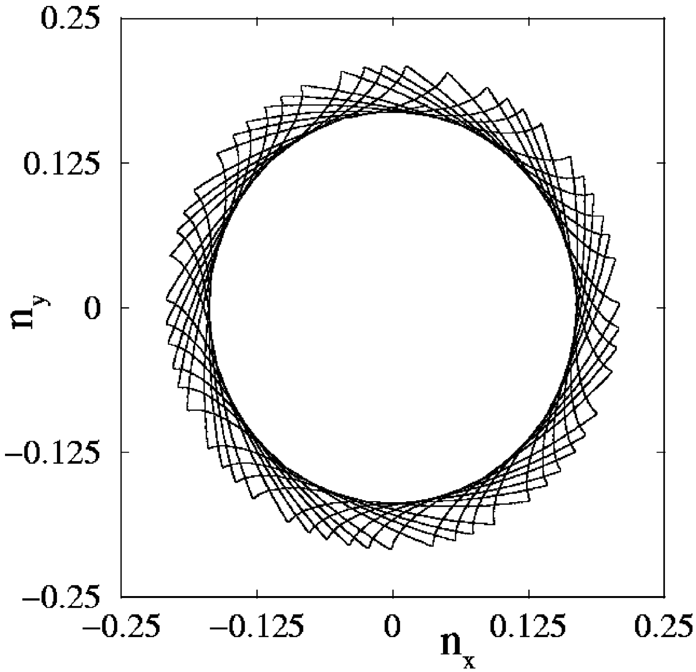

FIGURE 7 Trajectory in the (n_x, n_y) plane at $\rho = 1.55$.

amplitudes of the peaks decay quite fast with increasing n and only first few peaks are important. In Figures 5 and 6 the spectra of the director and output intensities for $\rho = 1.55$ are depicted. It should be noted that the amplitudes of the higher-order peaks relative to the main peak at $f = f_0$ (or $f = f_0^E$ for the output intensities) grows with increasing light intensity.

In Figure 7 the trajectory in the (n_x, n_y) plane is shown ($\rho = 1.55$). Whereas the trajectory in the laboratory frame (shown) is not closed, i.e., the motion of the director is quasiperiodic, the director performs a simple periodic motion with a frequency f_1 in the frame that rotates with a frequency f_0 around the z axis.

V. SECOND REGIME OF UNIFORM DIRECTOR PRECESSION

In some narrow region around $\rho_3 \approx 1.75$ the period $T = 1/f_1$ of the NUP increases progressively with increasing light intensity, and indeed appears to diverge logarithmically at ρ_3, with a best fit $T \propto -0.62 \ln(\rho_3 - \rho)$ (see Fig. 8). At $\rho = \rho_3$ the system jumps to a new state of uniform

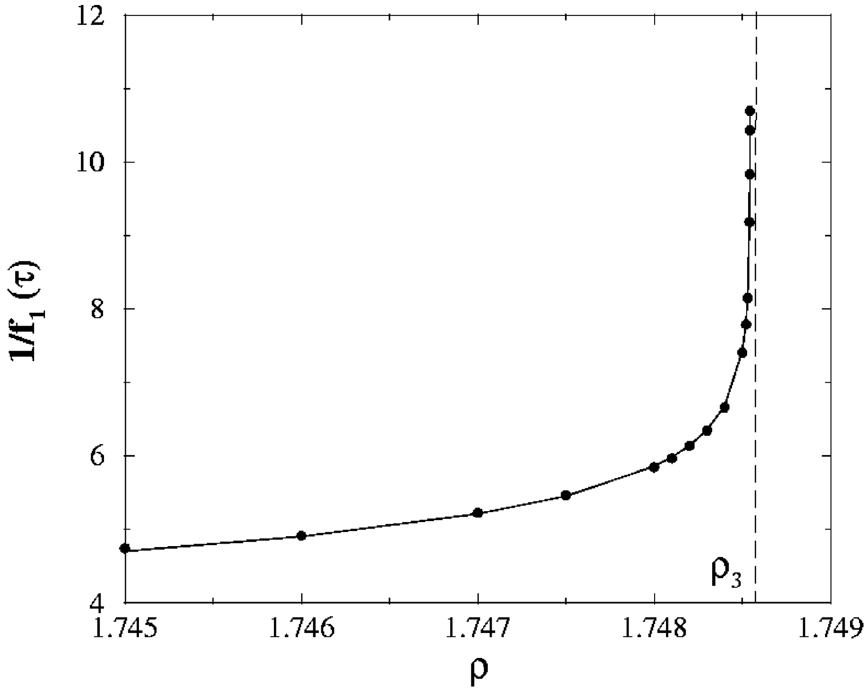

FIGURE 8 Dimensionless period $T = 1/f_1$ versus ρ near the limit $\rho = \rho_3$. The solid line is the best fit by a logarithmically diverging function (see text).

precession of the director (UP2) with large reorientation ($\theta \sim 74°$). The nature of the singularity at $\rho = \rho_3$ signifies that the discontinuous transition from NUP to UP2 has the character of a homoclinic bifurcation.

In Figure 9 $max_t|n_x, n_y|$ versus intensity ρ is depicted for the UP2 regime. Following the UP2 branch to lower intensities one finds a large and rather complicated hysteretic cycle, which eventually leads to a jump back to the UP1 regime at $\rho_3^* = 1.09$, see Figure 9. The left part of the UP2 branch consists of alternatively stable and unstable regions exhibiting a series of saddle-node bifurcations. This result was already obtained in the framework of an approximate model [3]. As is seen from Figure 9, at $\rho = \rho_3$ the unstable part of the UP2 state approaches very closely the NUP branch. This indicates that at $\rho = \rho_3$ the NUP becomes homoclinic to the unstable UP2 solution. We have checked that this vicinity relates to all components of the spatial modes (θ_n, φ_n), [$n = 1, \ldots$], i.e., to the full space-time solutions.

The minimal description of the full scenario of the UP2 and UP1 regimes within our framework involves two modes for (θ,φ), and two iterations for

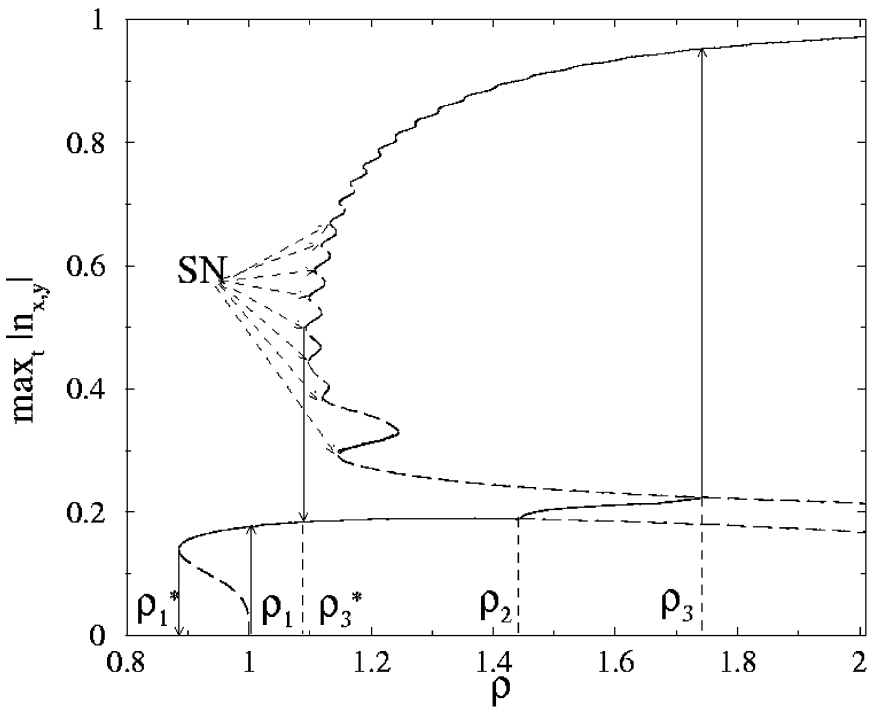

FIGURE 9 The maximum of the director components n_x, n_y with respect to t at point $z = \pi/2 - 0.1$ inside the nematic layer versus normalized intensity ρ. Solid (dashed) lines are stable (unstable) solutions. At $\rho = \rho_1$: transition to the first regime of uniform director precession; at $\rho = \rho_1^*$: switch back to the homeotropic state; at $\rho = \rho_2$: transition to the regime of nonuniform director precession; at $\rho = \rho_3$: transition to the second regime of uniform director precession; at $\rho = \rho_3^*$: switch back to the first regime of uniform director precession. SN: a series of saddle-node bifurcations.

A_o, A_e. One then obtains an accuracy comparable to that of the model presented in [3].

The phase diagram in (n_x, n_y) plane is represented by a simple circle for the UP2 states (as for the UP1 case). Also the Fourier spectrum of $n_{x,y}$ and $|E_{x,y}|^2$ for the UP2 regime has the same structure as for UP1. However, the period of director precession is several orders of magnitude larger than that in the UP1 and NUP regimes. At isolated points of the light intensity the period can even become infinite, i.e., the limit cycle degenerates to a continuum of the fixed points on the circle, although it cannot reverse. This can be understood from the reduced model [3], where the authors presented an approximate formula for the frequency $f_0 \sim |(\cos\delta - 1)/\delta|$, where δ is the phase delay introduced in sec. III. It is seen from this formula that f_0 can indeed touch zero with growing δ. For the UP1 and NUP regimes δ is always smaller than 2π, whereas for the UP2 regime the values of δ vary over a wide region from $\sim 2\pi$ to many times of 2π.

VI. CONCLUSIONS

We have studied theoretically the transitions induced by circularly polarized light incident perpendicularly to a layer of nematic liquid crystal that has initially homeotropic alignment. In our work we started from the standard equations of motion for the director coupled to the equations for the amplitudes of the ordinary and extraordinary light that were solved iteratively. Our numerical analysis of the problem shows that the one-mode approximation for the polar angle θ (which is one of the assumptions made in previous work [3]) is fairly accurate for both, the UP1 and UP2 regime. Adding higher modes on the polar angle θ does in our approach not give an appreciable change in the dynamical picture. However, the simple model introduced in [3] cannot predict the NUP regime. Recently the NUP regime was studied experimentally and theoretically [4,5] without, however, resolving the detailed bifurcation structure.

We have explored the three types of the director instabilities in detail. With increasing light intensity, the first instability corresponds to the transition from the homeotropic orientation to a state where the director performs a uniform precession around the direction of propagation of the light. This state destabilizes via a supercritical Hopf bifurcation and a new frequency f_1 in the Fourier spectra of the director and of the output intensities appears. This regime corresponds to nonuniform director precession with nutation. As the intensity increases further, this state disappears at a certain critical value. At this intensity the period of nutation $T = 1/f_1$ becomes infinite and a discontinuous transition to a state with large reorientation occurs via a homoclinic bifurcation. The new state again corresponds to a uniform precession of the director, however, with very large period.

REFERENCES

[1] Santamato, E., Daino, B., Romagnoli, M., Settembre, M., & Shen, Y. R. (1986). *Phys. Rev. Lett.*, *57*, 2423.
[2] Santamato, E., Romagnoli, M., Settembre, M., Daino, B., & Shen, Y. R. (1988). *Phys. Rev. Lett.*, *61*, 113.
[3] Marrucci, L., Abbate, G., Ferraiuolo, S., Maddalena, P., & Santamato, E. (1992). *Phys. Rev. A 46*, 4859.
[4] Brasselet, E., Doyon, B., Galstian, T. V., & Dube, L. J. (2002). *Phys. Lett. A 299*, 212.
[5] Brasselet, E., Doyon, B., Galstian, T. V., & Dube, L. J. (2003). *Phys. Rev. E 67*, 031706.

[6] Santamato, E. & Shen, Y. R. (1987). *J. Opt. Soc. Am. A 4*, 356.
[7] de Gennes P. G. & Prost, J. (1993). *The physics of liquid crystals*, Clarendon press: Oxford.
[8] Vella, A., Piccirillo, B., & Santamato, E. (2002). *Phys. Rev. E 65*, 031706.
[9] Marrucci, L., Paparo, D., Vetrano, M. R., Colicchio, M., Santamato, E., & Viscardi, G. (2000). *J. of Chem. Phys.*, *113*, 10361.
[10] Gipparrone, G., Duca, D., Versace, C., Umeton, C., & Tabiryan, N. V. (1995). *Mol. Cryst. Liq. Cryst. Sci. Technol., Sec A 266*, 263.